Published in final edited form as:
Neuroreport. 2005 April 4; 16(5): 463–467.

Cortical Reorganization in Children with Unilateral Sensorineural Hearing Loss

Vincent J. Schmithorst, Ph.D.[1], **Scott K. Holland, Ph.D.**[1], **Jennifer Ret**[1], **Angie Duggins**[2], **Ellis Arjmand, M.D.**[2], and **John Greinwald, M.D.**[2]

1*Imaging Research Center, Children's Hospital Medical Center, Cincinnati, OH*

2*Center for Hearing and Deafness Research, Children's Hospital Medical Center, Cincinnati, OH*

Abstract

Previous studies have shown evidence of cortical reorganization following unilateral sensorineural hearing loss (USNHL). In addition, subjects with right USNHL have shown greater deficits in academic and language performance compared to subjects with left USNHL. A preliminary functional MRI investigation was performed on a small cohort of subjects, 4 with left USNHL and 4 with right USNHL, using the paradigm of listening to random tones. While the subjects with left USNHL displayed greater activation in the right superior temporal gyrus, the subjects with right USNHL displayed greater activation in the left inferior frontal area immediately anterior to the superior temporal gyrus. The results provide preliminary evidence of disparate neural circuitry supporting auditory processing in subjects with left and right USNHL.

Keywords

Hearing Loss; Sensorineural/Unilateral; Child Behavior Disorders; Brain Mapping; Auditory Perception; Magnetic Resonance Imaging

Introduction

It has been estimated that approximately 25 out of every 1,000 school-aged children in the United States suffer from hearing losses that may significantly interfere with their education [1,2]. Of the affected children, over two-thirds suffer from unilateral, as opposed to bilateral, hearing loss [2]. Fully one percent of school-aged children have a hearing loss which is severe-to-profound in severity [3].

Children with unilateral sensorineural hearing loss (USNHL) have shown deficits in such areas as speech recognition [4], sound localization [5], and academic performance [6,7]. The risk of academic failure has been shown to be significantly greater in subjects with right USNHL as compared to subjects with left USNHL [8,9]. A better understanding of the compensatory strategies used in children with USNHL, especially regarding cortical reorganization and neuroplasticity, could potentially be helpful in the designing of effective treatment and management strategies.

Various studies have shown reorganization of auditory and language pathways in patients with USNHL. In subjects undergoing monaural stimulation, normal-hearing subjects displayed activation lateralized to the contralateral side, while unilaterally deaf subjects displayed

Correspondence to: Vincent J. Schmithorst, Ph.D., Imaging Research Center, Children's Hospital Medical Center, 3333 Burnet Ave. ML 5031, Cincinnati, OH 45229, Tel: (513) 636-3922, Fax: (513) 636-3754, e-mail: Vince.Schmithorst@cchmc.org.

bilateral activation patterns [10,11], indicating a functional reorganization of auditory pathways [12]. Previous studies also support the idea that the neural correlates of language and auditory processing vary with exposure to various language and environmental stimuli during the developmental period. For instance, activation in the left lateral temporal cortex was significantly reduced in a congenitally deaf population relative to normal controls during a speech-reading task [13], indicating that early acoustic experience may be necessary for specific speech analysis functionality to develop in certain brain regions.

Thus, the ability of pediatric subjects with USNHL to compensate may depend greatly on the treatment and management approach; specifically, whether that approach fosters or hinders the optimal functional reorganization of auditory and language pathways. This reorganization, however, may differ in subjects with right and left USNHL, as evidenced by the “right-ear advantage” in early childhood. We performed a preliminary investigation of this hypothesis using functional MRI (fMRI).

Materials and Methods

Subjects were recruited from the Center for Hearing and Deafness Research at Cincinnati Children's Hospital Medical Center. Institutional Review Board approval was obtained for the study, and informed consent was obtained from the subjects’ parents, with assent obtained from the subjects themselves when appropriate. Subjects were diagnosed as having USNHL with the worse ear having a mean Pure Tone Audiometry (PTA) air conduction threshold of greater than 65dB HL and no frequency better than 45dB HL at 500 to 4000 Hz, and a PTA of 15dB HL or less and no one frequency greater than 25dB HL for the better ear. All patients had ideopathic hearing loss with normal CT scans and no history of infections (i.e. meningitis or CMV), family history or trauma. FMRI data was obtained from nine subjects; however, the data from one subject was excluded due to gross motion artifacts. For the eight subjects (4M, 4F, age [mean ± σ] = 9 ± 1.8 years)) remaining, 4 had right SNSHL and 4 had left USNHL. The youngest subject was 7 years old, and the oldest subject was 12 years old. There was not a significant difference in the mean age (8.5 years) of the subjects with right USNHL and the mean age (9.5 years) of the subjects with left USNHL ($p > 0.45$, student’s T-test).

All subjects were scanned using a Bruker 3T Medspec system. Imaging parameters used for the echo-planar imaging (EPI)-fMRI scans were: TR = 3000 ms, TE = 38 ms, FOV = 25.6 X 25.6 cm, imaging matrix = 64 X 64, bandwidth = 125 kHz. Twenty-four slices of thickness 5 mm were imaged, covering almost the whole brain. A block-design (30 seconds active, 30 seconds rest) paradigm was used. During the active periods the subjects listened to pure tones of random duration (range 200 ms – 2 s) and frequency (range 400 Hz – 3 kHz) presented continuously through an MR-compatible audio system (Model SS3100, Avotec Inc., Stuart, FL). This system comprises a pneumatic stereo headset driven by stereo voice coil transducers, optimally acoustically coupled to a tuned length of high density, reinforced, tygon tubing. The system was calibrated by the manufacturer using a B&K 2230 sound level meter to measure the sound pressure level (SPL) at the ear pieces in one-third octave bands from 250 Hz to 4kHz. A balanced, flat frequency response was achieved at the ear pieces by adjusting the frequency response at the input to the transducers using a JVC octave band equalizer included with the system. This resulted in a measured, flat frequency response from 250 Hz to 4kHz, and balance between the left and right channels. The Avotec SS3100 was used for these experiments in preference to other MRI audio systems available in our laboratory because of the high audio amplitude capability of this system. With the calibrated SS3100 we could produce SPL = 120 dBA at each ear piece. This capability was desirable in order to insure that we could be able to stimulate deaf subjects at levels exceeding measured hearing levels.

Subjects were instructed prior to the scanning session to pay attention to the stimuli but not to make any explicit responses. The particular paradigm was selected due to the relative ease of hearing the stimuli over the background scanner noise (of constant frequency ~1 kHz), and the volume was set to approximately 10 dBA above the measured hearing level of the good ear so that the subjects reported clearly hearing the stimuli. 11 epochs (6 rest, 5 active) were obtained, for a total scan time of 5 minutes 30 seconds. Data from the first (rest) epoch was discarded in order to allow the spins to reach relaxation equilibrium. In addition, a high-resolution whole-brain T1-weighted anatomical image was acquired for the purpose of anatomical coregistration.

The fMRI data was post-processed using routines written in IDL (Research Systems Inc., Boulder, CO). Geometric distortion in the EPI images was corrected for using a multiecho reference scan [14]. Motion correction was performed using a pyramid iterative algorithm [15], and the motion-corrected data was then transformed into stereotaxic (Talairach) space using landmarks obtained from the T1-weighted anatomical images. For each subject, on a voxel-by-voxel basis, percent change maps were calculated from the average signal intensities in the control and active periods ($\%\ \text{change} = \frac{\mathcal{A} - \mathcal{C}}{\mathcal{C}} * 100\ \%$ where $\mathcal{A}$ and $\mathcal{C}$ are the mean MRI signal intensities in the active and control epochs, respectively. The first three frames following the transition were discarded in order to account for the delay in the hemodynamic response. In addition, only those frames were included in the analysis for which the maximum voxel displacement due to subject motion was found to be less than 3 mm. Since the maximum voxel displacement is found at the corner of the image volume, the typical displacement for most voxels in the brain would be less than 2 mm. If this criterion did not result in at least 15 usable frames for both resting and active periods, the entire dataset was discarded, resulting in usable data from only 8 out of the 9 subjects scanned.

Voxelwise random-effects analyses were then performed on the percent change maps. Percent-change, rather than effect size, was selected as the dependent variable for several reasons. In this small cohort including subjects as young as seven years old, the number of usable frames varied across subjects, and the standard deviation used to compute the effect size is dependent on the number of frames used in the analysis. In addition, since the standard deviation is not only subject dependent, but also brain region dependent, percent change will likely be a more suitable measure to use in order to compare activation intensities across regions.

The analysis was first restricted to those voxels with a mean percent change (across subjects) of 0.25% or greater. A within-group analysis was performed (Figure 1). (Figure 1 near here). Incorporating the estimated intrinsic smoothness of the data, the exogenous spatial filter width of 4 mm, the chosen threshold of $Z > 6.0$, and cluster size of 10 resulted in a corrected double-tailed $p < 0.001$/cluster found via Monte Carlo simulation. For the subset of voxels found to be active using the within-group analysis, a between-groups (left USNHL vs. right USNHL) analysis was performed (Figure 2). (Figure 2 near here). Due to the small sample size, age was not incorporated as a covariate, as no significant difference in age was found between the two groups; however, a non-parametric Spearman correlation was used, in order to account for possible variations from normality, with the p-values from the correlation converted into Z-scores. The spatial filter width of 7 mm, threshold of $Z > 6.0$, and cluster size of 25 resulted in a corrected double-tailed $p < 0.05$/cluster for the region (right superior temporal gyrus) exhibiting activation in subjects with left USNHL > activation in subjects with right USNHL. A smaller cluster (left inferior frontal gyrus) with activation in subjects with right USNHL > subjects with left USNHL did not quite reach significance but had double-tailed $p < 0.10$. The foci of activation for the within-group analysis, and of differences for the between-group analysis, are listed in Tables 1 and 2, respectively. (Tables 1 and 2 near here.) For the significant voxels for the regions listed in Table 2, the average percent change was calculated for both areas and is displayed in Figures 3 and 4, for both subject cohorts. (Figures 3 and 4 near here.)

The Monte Carlo simulations used to estimate corrected p-values were performed in the following manner, based on the method of Ledberg *et al*. [16]. The spatial autocorrelations present in the fit residuals were used to estimate the intrinsic smoothness in the data. "Null" activation maps were generated from spatially autocorrelated Gaussian noise generated using the previously found smoothness estimates and postprocessing parameters (e.g. threshold intensity, cluster size, and exogenous spatial filtering). The simulations were repeated, and the corrected p-values estimated by computing the proportion of null maps with spurious activated clusters detected.

Results and Discussion

Robust activation was found in the auditory cortex bilaterally (Figure 1). However, there is unexpected activation in the inferior frontal gyrus bilaterally, as well as the cuneus. These results might represent a general cortical reorganization strategy present in subjects with USNHL on either side, although additional research will be necessary to verify this hypothesis.

The cohort with left USNHL displayed significantly greater activation in the right superior temporal gyrus, and this finding is extremely robust (Figure 3), even with our small sample size. Using a published probability atlas, the focus of this area was found to be in Heschl's gyrus (BA 41), and not the planum temporale (BA 22). This result is unexpected, as one might expect the activation from the intact contralateral auditory pathway to the right superior temporal gyrus in subjects with right USNHL to be at least equal or perhaps stronger than the activation from the ipsilateral pathway formed after cortical reorganization in subjects with left USNHL.

One possible interpretation is that these findings represent greater central auditory reorganization to the right hemisphere in children with left USNHL, consistent with the bilateral representation of auditory processing in subjects with USNHL found previously [17]. Is the "right-ear advantage" simply due to increased bilateral representation in subjects with left USNHL? To investigate this hypothesis further, the average signal change in the left superior temporal gyrus was computed by mirroring the voxels (i.e. using the negative left-right Talairach coordinates) found in the right superior temporal gyrus. No significant activation difference was found in the left superior temporal gyrus (Spearman's $R = 0.11$; $p > 0.75$) between subjects with right and left USNHL. In addition, 1 out of the 4 subjects with right USNHL, and 2 out of the 4 subjects with left USNHL displayed significantly greater activation on the ipsilateral side (Student's t-test, $p < 0.05$ double-tailed) while none of the subjects displayed greater activation on the contralateral side to the hearing ear; there was no significant difference however in ipsilateral dominance between the two groups (Spearman's $R = 0.33$; $p > 0.4$).

Our results therefore, while preliminary and limited by the small sample size, do not support the hypothesis of greater bilateral auditory representation in itself being the neural basis for the right-ear advantage. While the superior temporal area with greater activation in subjects with left USNHL is located in the right hemisphere primary auditory area, the inferior frontal area with a trend to greater activation in subjects with right USNHL (Figure 2) is located anterior to left hemisphere primary auditory areas. This leads us to propose the hypothesis that the cortical reorganization in the hemisphere ipsilateral to the hearing ear differs in subjects with left and right USNHL, with reorganization towards superior temporal areas in subjects with left USNHL and towards inferior frontal areas in subjects with right USNHL. While our results in this region were not as robust (Figure 4), only reaching a trend with our small sample size, a wide variance is evident, with two out the four subjects with right USNHL displaying extremely robust activation in this region. Those two subjects were the youngest of the four, both seven years of age.

Based on our findings in this small sample of children with USNHL we can speculate the following neural basis for the “right-ear advantage”. An early cortical reorganization occurs in subjects with right USNHL towards left frontal areas, with the contralateral pathways for language processing having been disrupted. However, these areas become more relevant for language processing with increasing age, as language function becomes more left-lateralized [18], necessitating an additional cortical reorganization of ipsilateral auditory pathways. Further research, involving a longitudinal study of children with USNHL, will help to verify the preceding hypothesis. Preliminary studies in children with left perinatal infarction of the middle cerebral artery (MCA) also suggest that early interference with typical auditory and language pathways in the cerebral cortex will result in reorganization to ipsilateral regions when available [19]. To the extent that left hemisphere language regions are spared from injury following left MCA infarction, the developing brain tends to utilize remaining left dominant regions for auditory and language processing.

In previous studies (e.g. [20]) performed on normal-hearing adult subjects, the presentation of monaural stimuli has produced a contralaterality effect in the superior temporal gyrus. This asymmetric cortical response has been attributed to differences in anatomical organization. Crossing auditory pathways may have a greater number of fibers and faster transmission speed relative to ipsilateral pathways [21]. In contrast, 3 out of 8 subjects displayed greater activation on the side ipsilateral to the better-hearing ear, with no subjects displaying a contralaterality effect. Thus, the hypothesized cortical reorganization may also be associated with changes in fiber organization, as white matter maturation has been observed to continue throughout the developmental period [22]. Future research involving diffusion tensor imaging (DTI) may investigate this possibility in more detail.

The changes in cortical representation in children with UNSHL may stem from bottom-up or top-down mechanisms. For normal-hearing subjects undergoing monaural stimulation, the resultant shift in attentional focus may be a mechanism resulting in enhancement of activation in the contralateral auditory cortex [20]. Thus habituation to attentional effects is a possible explanation for our failure to find contralaterality in children with UNSHL. On the other hand, the existence of a top-down bihemispheric regulatory mechanism adjusting the symmetric auditory input has also been proposed, which may also result in a trend towards bilateral representation in patients with UNSHL, as has been observed for adults with a sudden onset of UNSHL [12]. Further research will be necessary to elucidate the precise mechanisms responsible for cortical reorganization in children with UNSHL.

A significant limitation of this preliminary study is that it was not known whether there was any residual cortical activity from auditory pathways in the deaf ear. It is extremely difficult to present auditory stimuli able to be heard in an ear with severe-to-profound hearing loss over the scanner noise, which is approximately 110–120 dBA on our 3T system [23] for an EPI sequence. Conversely, it is very likely that some auditory stimulation occurred due to the scanner noise itself, even in the deaf ear. Future studies will incorporate a recently developed sequence with silent gradient intervals [24] suitable for use in a hearing-impaired pediatric population.

Conclusion

A preliminary investigation of possible differences in cortical reorganization in subjects with left USNHL versus subjects with right USNHL was performed using the fMRI paradigm of listening to random tones. Subjects with left USNHL displayed greater activation in the right primary auditory cortex, while subjects with right USNHL displayed greater activation in the left inferior frontal gyrus immediately anterior to the auditory cortex. The results may indicate differing cortical reorganization in patients with left and right USNHL, although they do not

support an explanation for the “right-ear advantage” based on greater bilateral auditory representation.

References

1. Bess FH. The minimally hearing-impaired child. Ear Hear 1985;6:43–47. [PubMed: 4038669]
2. Lundeen C. Prevalence of hearing impairment among children. Language, Speech, and Hearing Services in Schools 1991;22:269–271.
3. Schein J, Delk M. The deaf population of the United States. Silver Spring, MD: National Association of the Deaf, 1974.
4. Kenworthy OT, Klee T, Tharpe AM. Speech recognition ability of children with unilateral sensorineural hearing loss as a function of amplification, speech stimuli and listening condition. Ear Hear 1990;11:264–270. [PubMed: 2210100]
5. Bess FH, Tharpe AM, Gibler AM. Auditory performance of children with unilateral sensorineural hearing loss. Ear Hear 1986;7:20–26. [PubMed: 3949097]
6. Klee TM, Davis-Dansky E. A comparison of unilaterally hearing-impaired children and normal-hearing children on a battery of standardized language tests. Ear Hear 1986;7:27–37. [PubMed: 3949098]
7. Bess FH, Tharpe AM. Unilateral hearing impairment in children. Pediatrics 1984;74:206–216. [PubMed: 6462820]
8. Bess FH, Tharpe AM. Case history data on unilaterally hearing-impaired children. Ear Hear 1986;7:14–19. [PubMed: 3949096]
9. Oyler RF, Oyler AL, Matkin ND. Warning: A unilateral hearing loss may be detrimental to a child's academic career. The Hearing Journal 1987;40:18–22.
10. Scheffler K, Bilecen D, Schmid N, Tschopp K, Seelig J. Auditory cortical responses in hearing subjects and unilateral deaf patients as detected by functional magnetic resonance imaging. Cereb Cortex 1998;8:156–163. [PubMed: 9542894]
11. Tschopp K, Schillinger C, Schmid N, Rausch M, Bilecen D, Scheffler K. [Detection of central auditory compensation in unilateral deafness with functional magnetic resonance tomography]. Laryngorhinootologie 2000;79:753–757. [PubMed: 11199459]
12. Vasama JP, Makela JP, Pyykko I, Hari R. Abrupt unilateral deafness modifies function of human auditory pathways. Neuroreport 1995;6:961–964. [PubMed: 7632899]
13. MacSweeney M, Campbell R, Calvert GA, McGuire PK, David AS, Suckling J, et al. Dispersed activation in the left temporal cortex for speech-reading in congenitally deaf people. Proc R Soc Lond B Biol Sci 2001;268:451–457.
14. Schmithorst VJ, Dardzinski BJ, Holland SK. Simultaneous correction of ghost and geometric distortion artifacts in EPI using a multiecho reference scan. IEEE Trans Med Imaging 2001;20:535–539. [PubMed: 11437113]
15. Thévenaz P, Unser M. A Pyramid Approach to Subpixel Registration Based on Intensity. IEEE Transactions on Image Processing 1998;7:27–41.
16. Ledberg A, Akerman S, Roland PE. Estimation of the probabilities of 3D clusters in functional brain images. Neuroimage 1998;8:113–128. [PubMed: 9740755]
17. Ponton CW, Vasama JP, Tremblay K, Khosla D, Kwong B, Don M. Plasticity in the adult human central auditory system: evidence from late-onset profound unilateral deafness. Hear Res 2001;154:32–44. [PubMed: 11423213]
18. Holland SK, Plante E, Weber Byars A, Strawsburg RH, Schmithorst VJ, Ball WS Jr. Normal fMRI Brain Activation Patterns in Children Performing a Verb Generation Task. Neuroimage 2001;14:837–843. [PubMed: 11554802]
19. Schapiro MB, Wakefield JL, Byars AW, Schmithorst VJ, Strawsburg RH, Holland SK. Functional magnetic resonance imaging reveals atypical language organization in children following perinatal left middle cerebral artery stroke. Ann Neurol 2003;54:S109.
20. Jancke L, Wustenberg T, Schulze K, Heinze HJ. Asymmetric hemodynamic responses of the human auditory cortex to monaural and binaural stimulation. Hear Res 2002;170:166–178. [PubMed: 12208550]

21. Majkowski J, Bochenek Z, Bochenek W, Knapik-Fijalkowska D, Kopec J. Latency of averaged evoked potentials to contralateral and ipsilateral auditory stimulation in normal subjects. Brain Res 1971;25:416–419. [PubMed: 5545728]

22. Schmithorst VJ, Wilke M, Dardzinski BJ, Holland SK. Correlation of White Matter Diffusivity and Anisotropy Changes with Age During Childhood: A Cross-Sectional Diffusion Tensor Imaging Study. Radiology 2002;222:212–218. [PubMed: 11756728]

23. Hartnick CJ, Rudolph C, Willging JP, Holland SK. Functional magnetic resonance imaging of the pediatric swallow: imaging the cortex and the brainstem. Laryngoscope 2001;111:1183–1191. [PubMed: 11568539]

24. Schmithorst VJ, Holland SK. Event-related fMRI technique for auditory processing with hemodynamics unrelated to acoustic gradient noise. Magn Reson Med 2004;51:399–402. [PubMed: 14755667]

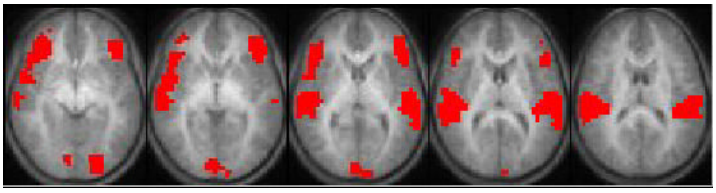

Figure 1.
Activation map displaying regions of significant activation for subjects with USNHL listening to random tones. Five slices selected for display (Z = −5 to +15 mm). All images in radiological orientation.

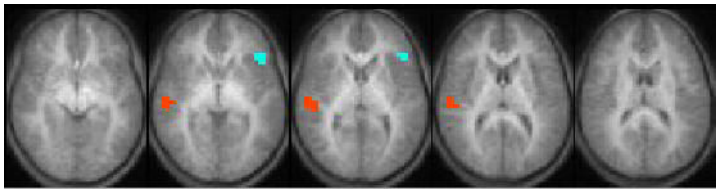

Figure 2.
Map displaying regions of activation differences between subjects with left and right USNHL (blue = right USNHL > left USNHL, red = left USNHL > right USNHL). Five slices selected for display (Z = −5 to +15 mm). All images in radiological orientation.

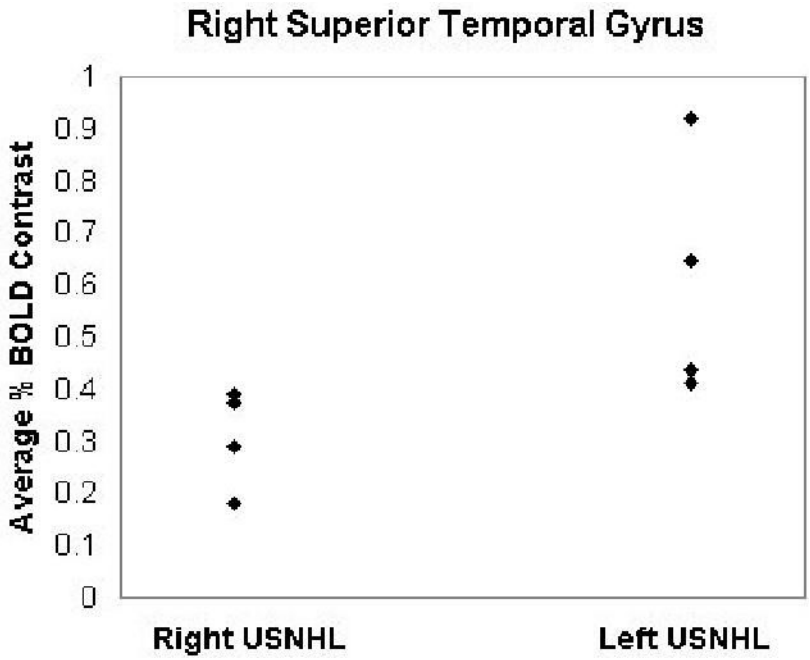

Figure 3.
Plot of average BOLD signal changes for subjects with left and right USNHL, for the right superior temporal gyrus (region outlined in Figure 2).

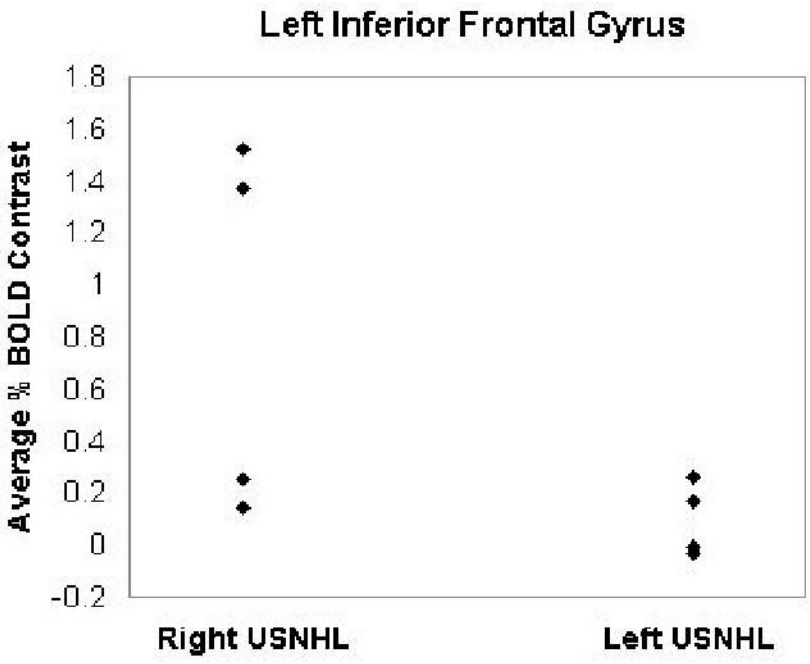

Figure 4.
Plot of average BOLD signal changes for subjects with left and right USNHL, for the left inferior frontal gyrus (region outlined in Figure 2).

Table 1

Talairach coordinates (X, Y, Z) and Brodmann's areas (BA) for the activation foci found in Figure 1. All regions have $p < 0.001$ (corrected).

X, Y, Z	BA	Anatomical Area
−58, −33, 5	22	L. Superior Temporal Gyrus
58, −17, 5	41	R. Superior Temporal Gyrus
−46, 39, −5	47	L. Inferior Frontal Gyrus
34, 23, −5	47	R. Inferior Frontal Gyrus
6, −89, 5	17	R. Cuneus
−22, −89, −5	18	L. Cuneus

Table 2

Talairach coordinates (X, Y, Z) and Brodmann's areas (BA) for the regions with significant differences between subjects with right and left USNHL found in Figure 2.

X, Y, Z	BA	Anatomical Area
54, −25, 5	41	R. Superior Temporal Gyrus*
−42, 23, 0	47	L. Inferior Frontal Gyrus†

*=$p < 0.05$;

†= $p < 0.10$ double-tailed.